INTEGRATING SENTINEL-1 SYNTHETIC APERTURE RADAR AND CHIRPS DATA FOR UNDERSTANDING HEAVY PRECIPITATION AND FLOODING IN AN GIANG PROVINCE, VIET NAM

Ton Binh Minh*[1] and Shou-Hao Chiang[2]

[1]International Ph.D Program in Environmental Science and Technology, University System of Taiwan
Center for Space and Remote Sensing Research, National Central University
No. 300, Zhongda Rd., Zhongli District, Taoyuan City 32001, Taiwan
Email: tonbminh@gmail.com

[2]Associate Professor, Center for Space and Remote Sensing Research, National Central University
No. 300, Zhongda Rd., Zhongli District, Taoyuan City 32001, Taiwan
Email: gilbert@csrsr.ncu.edu.tw

KEY WORDS: Flood, Sentinel-1, CHIRPS, climate change, Mekong River Delta

ABSTRACT: Understanding the mechanisms of heavy precipitation and flooding is essential for effective climate change adaptation and response. The cloud-penetrating ability of microwaves makes Synthetic Aperture Radar (SAR) an ideal tool for providing weather-independent images for flood mapping. Climate Hazards Group InfraRed Precipitation with Station data (CHIRPS) is a land-only rainfall dataset that incorporates 0.05° resolution satellite imagery with in-situ station data to create gridded rainfall time series for various analysis applications. This study employs intensity images from Sentinel-1 satellites to generate flood maps and utilizes CHIRPS to derive heavy rainfall frequency. The segmentation technique is applied to distinguish between pre-existing standing water, recently flooded areas, and non-flooded regions within the study area. By combining SAR and CHIRPS data, this research yields valuable insights into the relationship between heavy rainfall and flood occurrences in An Giang province, Viet Nam. The escalating frequency of heavy precipitation correlates with an augmentation in local rainfall amounts, and a positive correlation emerges between heavy rainfall and the extension of flood-prone areas. While recognizing that flooding influences water flow from the upstream of the Mekong River, flooding discharges from neighboring areas, and tidal levels, the accelerated trend of urbanization has also played a significant role. The expansion of impervious surfaces contributes to the severity of deep floods and elevates flood potential in the region. Furthermore, this research affirms the effectiveness of SAR intensity image mapping for flood detection, and the integration of SAR and CHIRPS data furthers our understanding of heavy precipitation mechanisms. As the implications of climate change persist, the findings are crucial for developing sustainable flood management strategies, as well as enhancing resilience to climate-induced challenges in the Mekong River Delta region.

1. INTRODUCTION

Climate change exerts a multifaceted influence on precipitation patterns, ushering in changes in both intensity and frequency. The most immediate consequence of intensified precipitation is the heightened risk of flooding, as underscored by C2ES (2023). Alongside the looming specter of floods, heavy precipitation carries a gamut of potential repercussions, including crop damage, soil erosion, and an elevated flood risk borne from heavy precipitation (EPA, 2023).

The Mekong River Delta, Viet Nam nestled in a low-lying expanse, regularly finds itself submerged under the deluge of rainy seasons. The delta's climate adheres to a dichotomy of dry and rainy seasons, characteristic of a tropical monsoon regime, with the dry season spanning from December through April, and the rainy season drenching the land from May to the end of November. However, under the effects of climate change, climatic influencers, including phenomena like the El Niño Southern Oscillation (ENSO) inducing the precipitation distribution and amount across the region depend on a range of climatic drivers, e.g., El Niño Southern Oscillation (ENSO). A growing literature has mentioned that climate change has altered annual and seasonal patterns of precipitation along with its spatial distribution. Annual flooding also changed due to the climate change. In terms of human impact, floods emerge as the most formidable of natural disasters, as corroborated by Jonkman (Jonkman, 2005). Therefore, to understand the mechanism of heavy precipitation and flooding inundation is necessary.

The Mekong River Delta is divided into thirteen provinces, An Giang is on the north of the delta, an upstream province, and its boundary is shared with Cambodia, Dong Thap, Can Tho, and Kien Giang (Figure 1). Under the urbanization trend, non-permeable surfaces like pavement and concrete in the urban areas in An Giang province have been expanded in recent

years. Therefore, the runoff during heavy rainfall events ability has also increased. In addition, the development of high-dyke systems for rice cultivation specificity areas also caused the increase in flooding in this area.

The Google Earth Engine (GEE) stands as an open-access gateway to an expansive repository of geospatial data, bolstered by the ever-advancing capabilities of cloud computing. This synergy empowers researchers with the ability to conduct seamless analyses of extensive scientific measurements, eliminating the cumbersome need for extensive data downloads. Recent developments within GEE have seen the integration of high-resolution satellite imagery and meteorological datasets, marking a significant leap forward in our capacity to observe and understand Earth's surface dynamics. This breakthrough holds particular promise for applications demanding fine-scale precision, such as flood extent estimation, assessments of water and food security, and a myriad of other critical analyses.

The repercussions of climate change reverberate through our world, manifesting as a mosaic of heterogeneous precipitation patterns across both spatial and temporal scales. While the temporal aspect of precipitation can be grasped through ground-based gauge observations, inherent uncertainties persist within the gauge data, notably the sparse network's incapacity to discern mesoscale precipitation events (Dubey, Gupta, Goyal, & Joshi, 2021). In this context, radar technology emerges as a beacon of hope, operating independently of cloud coverage and weather conditions to bestow us with invaluable insights for refining precipitation estimation. As a result, it becomes the key to unveiling the intricate spatial variations within precipitation patterns, illuminating our understanding of this vital climatic phenomenon.

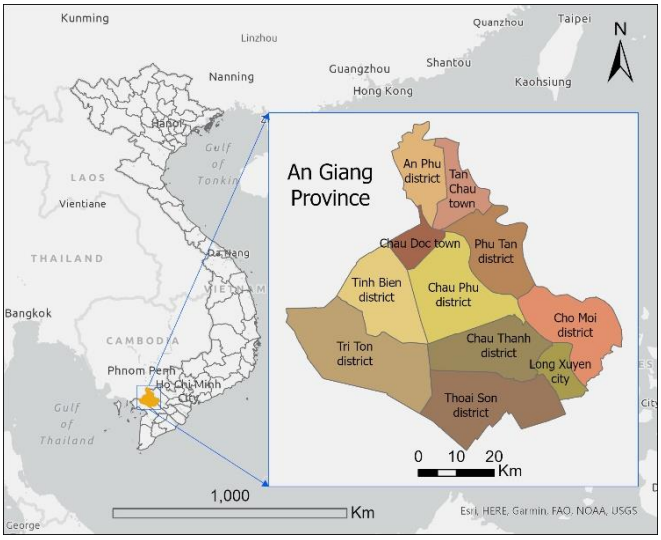

Figure 1. Location of An Giang province in Mekong River Delta, Viet Nam, and its administration districts. The background map is Esri's Light Gray Canvas basemap.

Recognizing the critical need to comprehensively evaluate precipitation characteristics, encompassing factors such as quantity, seasonality, variability, and long-term trends, within An Giang province under the effect of climate change, this study endeavors to delve into the spatial-temporal dynamics of heavy rainy days and flooding patterns spanning the period from 2018 to 2022. The primary objective of this research is to investigate significant changes in the occurrence of heavy precipitation events during the study period (2018-2022) relative to a robust 30-year baseline (1986-2015). Through this multifaceted analysis, this study aims to provide critical insights into the evolving climatic trends and their potential implications for the extent and severity of flooding in this area.

2. DATASETS

2.1 Gridded Rainfall Data

Within the vast repository of meteorological datasets accessible through the Google Earth Engine (GEE), the choice of the CHIRPS dataset for this study stands out due to its distinct advantages in spatio-temporal resolution and coverage, making it an indispensable tool for conducting a comprehensive precipitation analysis. Among the myriad of rainfall observations available on GEE, CHIRPS distinguishes itself with its superior spatio-temporal resolution, surpassing other available datasets (Banerjee et al., 2020; Dubey et al., 2021; Funk et al., 2015). CHIRPS boasts a daily record dating back to January 1, 1981, with a spatial resolution of 0.050 (approximately 5,566 meters) (Funk et al., 2015), enhancing its suitability for in-depth spatio-temporal rainfall analysis spanning over four decades. This strategic selection aligns with its widespread application in scientific research, evident in its integration into numerous studies focusing on precipitation

analysis and drought monitoring (Banerjee et al., 2020; Dubey et al., 2021). In this study, the CHIRPS daily dataset for the years 1983 to 2022 was harnessed to analyze the precipitation regime within the study area.

2.2 Sentinel-1

The Sentinel-1 missions orchestrated by the European Space Agency (ESA) offer a vital resource for acquiring weather-independent Earth observation data. Sentinel-1 employs a dual-polarization C-band Synthetic Aperture Radar (SAR) instrument operating at 5.405GHz, providing dataset scenes with spatial resolutions of 10, 25, and 40 meters, along with four band combinations, and three instrument modes. Each scene is equipped with one or two out of four possible polarization bands, depending on the polarization settings of the instrument. These bands include single-band VV (single co-polarization, vertical transmit/vertical receive) or HH (single co-polarization, horizontal transmit/horizontal receive), as well as dual-band VV+VH (dual-band cross-polarization, vertical transmit/horizontal receive), and HH+HV (dual-band cross-polarization, horizontal transmit/vertical receive) (Kramer, 2018). Furthermore, each scene features an angle band denoting the approximate incidence angle in degrees. Thanks to its C-band wavelength, Sentinel-1 imagery enables continuous monitoring of the earth's surface, facilitating the detection of changes regardless of short-term or long-term, day or night, and weather conditions. Notably, water bodies absorb this incident C-band wavelength, resulting in a low reflectance mode in Sentinel-1 VH band. Consequently, in this study, Sentinel-1 from 2018 to 2022, accessed via GEE, was leveraged for flood detection within the study area.

2.3 Other datasets

To enhance the precision of flood area estimation, two vital datasets, namely the Global Surface Water (GSW) dataset and the HydroSheds DEM dataset, were instrumental in excluding permanent water areas and regions with high-degree slopes. The GSW dataset offers comprehensive information, encompassing maps depicting the location and temporal distribution of surface water from 1984 to 2021, along with statistical insights into the extent and alteration of these aquatic surfaces (Pekel, Cottam, Gorelick, & Belward, 2016).

On the other hand, the HydroSheds DEM dataset, derived from elevation data collected by NASA's Shuttle Radar Topography Mission (SRTM) in 2000, provides a single elevation band at an approximate resolution of 93 meters. This dataset offers a diverse array of geo-referenced datasets at various scales, including river networks, watershed boundaries, and so on (Lehner, Verdin, & Jarvis, 2008). These datasets play a pivotal role in refining the accuracy of flood area extent estimations within the study area.

3. METHODS

3.1 Identification of Heavy Precipitation

Heavy precipitation is context-dependent due to varying regional norms. According to EPA (2023), heavy precipitation events are defined as instances in which rainfall or snowfall significantly exceeds typical levels. In this study, heavy precipitation is defined as the upper 10^{th} percentile. The analysis examines the proportion of total annual precipitation attributed to days with heavy precipitation. Essentially, it quantifies what percentage of precipitation occurs in a day. A heavy one-day event entails total precipitation that ranks within the upper echelons of the distribution of expected values for that location. Subsequently, days with a greater-than-normal proportion of precipitation from heavy precipitation events are identified, using the top 10^{th} percentile to establish a benchmark, resulting in an expected 10 percent baseline. This analysis is then aggregated on a provincial scale to determine the percentage of land area experiencing greater-than-normal precipitation from heavy precipitation events.

The CHIRPS daily precipitation dataset spanning from 1983 to 2022 served as the foundational resource for conducting a comprehensive analysis of precipitation patterns over a 40-year period. This analysis involved the computation of average monthly for 5-year intervals within this extended time frame, thereby allowing this study to discern variations in monthly precipitation across the study area. Furthermore, this study established two distinct periods, namely a long-term 30-year period (1986-2015) and the more recent 2018-2022 period. These periods were specifically delineated to facilitate the identification of heavy precipitation days by applying the percentile method and to calculate the disparities in rainfall between the five-year span of 2018-2022 and the long-term 30-year timeframe.

3.2 Flood Mapping

In this study, Sentinel-1 SAR data was harnessed through the GEE platform to meticulously monitor and detect flood events in the study area. The initial phase involved a refined data collection process, filtering images based on specific

criteria, including VH (vertical transmit and horizontal receive), IW instrument mode, descending and ascending orbit properties, and within 2018-2022. Subsequently, the composite images were generated, both pre-flood and flood events, and subjected to a speckle filter to effectively reduce noise.

To establish a baseline image before the flood event, images captured on 20 March 2018, during the dry season in the study area, were mosaicked and selected. The flood event images were derived from data collection between August to November from 2018 to 2022. Flood detection was achieved by quantifying the disparity in backscatter intensity between the pre-flood event and flood event images, employing a predefined threshold to delineate flooded regions, following the application of the Refined Lee filter method to remove speckle noise. Regions exhibiting pixel values indicating changes of greater than 25% were identified as flood areas.

In the pursuit of accuracy in the estimation of the flood extent, certain areas were excluded from the analysis. Permanent water bodies were identified using GSW dataset. Any pixel displaying a seasonality band of greater than 5 months was classified as permanence water. Additionally, high-degree slope areas were masked out using HydroSheds DEM dataset. Regions with slopes exceeding 5 degrees were considered to be subject to noise interference in the imagery. Furthermore, isolated pixels were mitigated through an isolated pixel mask, as single pixels detected in remote areas were likely to be noise. Pixels with fewer than 8 connected neighbors were systematically masked out. The resultant flood map was then utilized for statistical analysis of the flooded area and for visualization purposes.

4. RESULTS AND DISCUSSION

4.1 Spatio-Temporal Distribution of Precipitation

Over the 40-year period from 1983 to 2022, An Giang province experienced an average annual precipitation of 1469 mm, distributed across approximately 239 rainy days each year. However, this precipitation showed significant spatial variation and seasonality. To better understand these patterns, the rainfall characteristics of An Giang province have been categorized into four distinct regions based on long-term mean precipitation values, as illustrated in Figure 2(b). These regions are delineated as follows: zone-1, with an annual precipitation range of 1200-1400 mm; zone-2, experiencing rainfall between 1400 and 1600 mm annually; zone-3, characterized by a precipitation range of 1600-1800 mm; and finally, zone-4, which receives the highest annual rainfall of 1800-2000 mm. Notably, there is a discernible trend of decreasing rainfall from the southwestern to the northeastern parts of the province, with areas closer to the sea exhibiting higher precipitation levels compared to those farther inland. Zone-4, representing the highest rainfall levels, primarily encompasses the mountainous regions within the province.

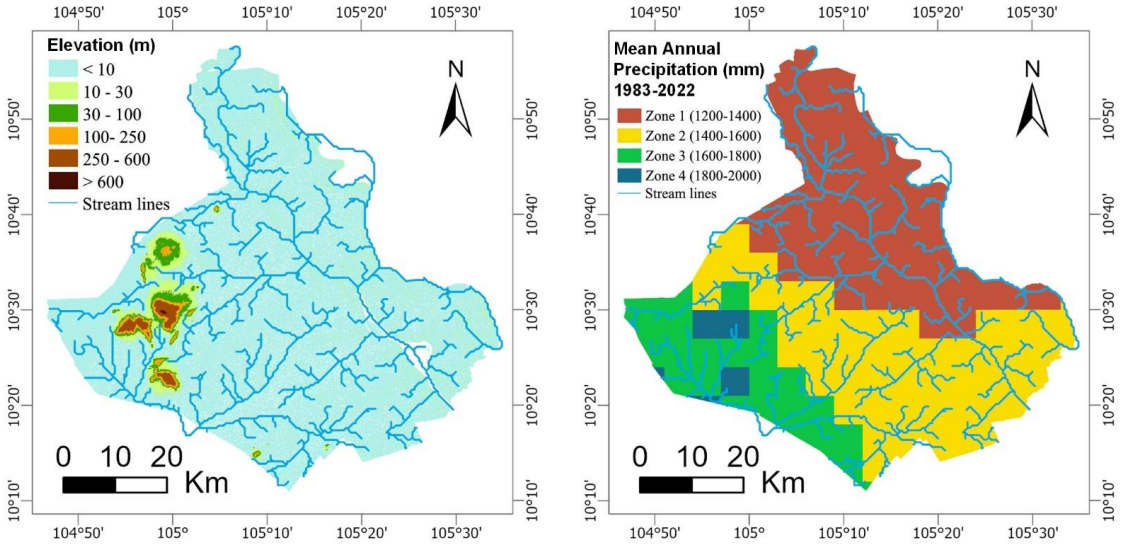

Figure 2. Generated elevation of An Giang from Shuttle Radar Topography Mission Digital Elevation Model (STRM DEM) 30 m and the streamlines from the HydroRIVERS (Lehner & Grill, 2013) (a). Precipitation regime zones from long-term mean annual rainfall from CHIRPS daily data and the streamlines from the HydroRIVERS; zone-1: 1200-1400 mm, zone-2:1400 - 1600 mm, zone-3: 1600-1800 mm, and zone-4: 1800–2000 mm (b).

In addition to understanding fluctuations in monthly precipitation, an annual precipitation cycle has been established by averaging monthly data over five-year intervals spanning four decades from 1983 to 2022 (Figure 3). Particularly, the amount of precipitation remains relatively low during the mid-months of the dry season, specifically in December, January,

and February. There is a discernible upward trend as the dry season progresses, particularly in March and April, culminating in the peak of precipitation during October. However, this peak is followed by a declining trend towards the end of the rainy season in November. While the precipitation curves within five-year periods exhibit similar shapes, variations in precipitation amounts among months are evident, notably towards the end of the dry season in April, and during the middle and end of the rainy season, particularly in July and October, respectively.

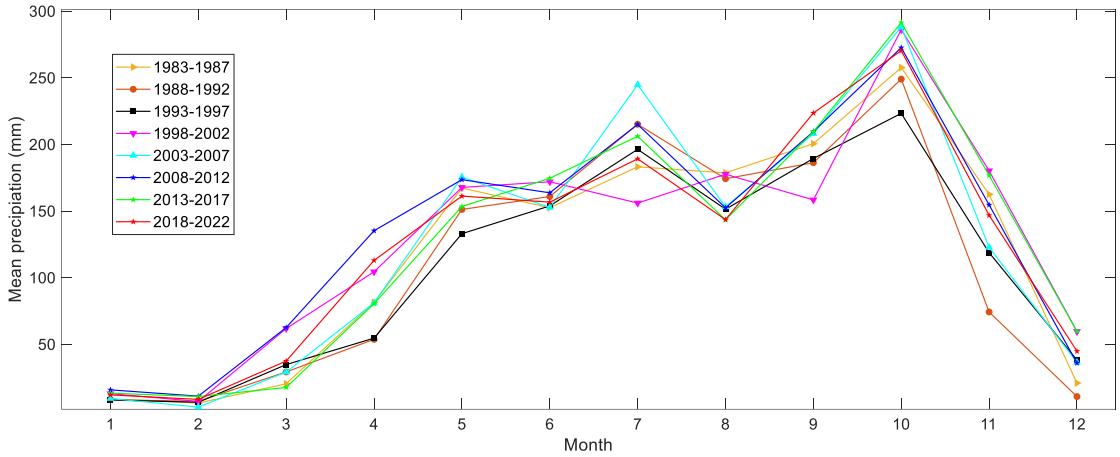

Figure 3: Average monthly precipitation of 5-year periods

All four regime zones had wet conditions mainly in May to November and dry conditions in December, January, February, March, and April. The long-term mean monthly rainfall (Figure 4) shows that July, August and September, and October were the main rainy months, while January, February, and March were the driest months, whereas rainfall was observed in December, April in the area.

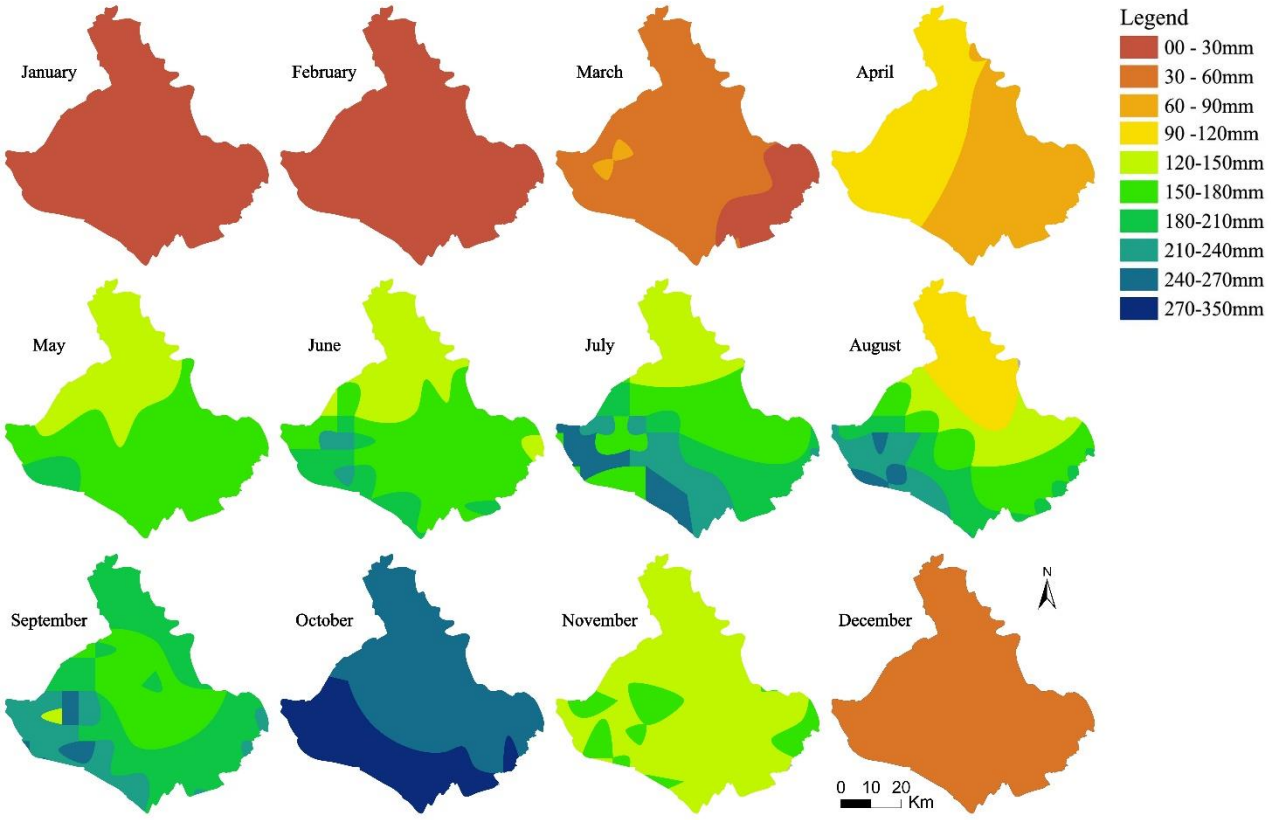

Figure 4. Spatial distribution of long-term mean monthly rainfall in 1983–2022 over the study area.

Figure 5 provides a comprehensive overview of monthly precipitation and the standard deviation of mean monthly rainfall across four distinct rainfall zones spanning the year 1983 to 2022. The data highlight the dynamic nature of precipitation, with each zone showcasing characteristic fluctuations throughout the months. This consistent pattern of

highs and lows is observed across all zones. For instance, in Zone 1, February records the lowest mean precipitation (approximately 6.33 mm), while October registers the highest (255.03 mm). Meanwhile, the standard deviations maintain seasonal trends, revealing non-uniformity in both months and regions. Notably, the rainy months (May to November) consistently exhibit elevated standard deviation, indicative of heightened variability in precipitation during these months. Intriguingly, upon calculating the average long-term standard deviation of monthly mean precipitation, October emerges as the month with the most pronounced variation in all zones, marked by a standard deviation of 8.60 approximately. Consequently, this study prompts a deeper investigation into the frequency of heavy precipitation events during this specific month.

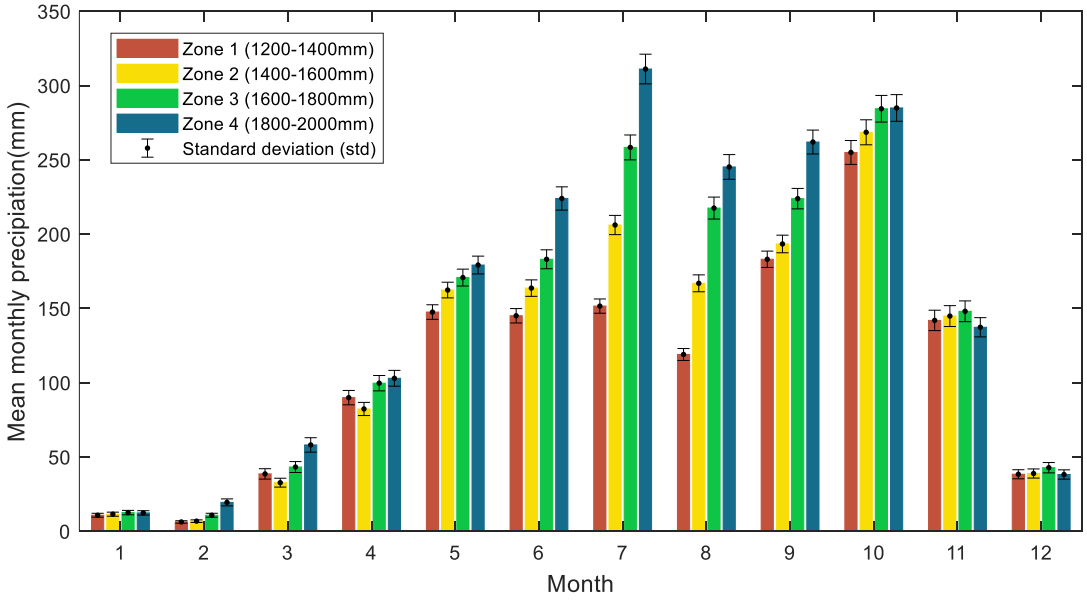

Figure 5. Mean monthly precipitation and standard deviation of mean monthly rainfall in 1983-2022 over the four rainfall zones

4.2 Identify the Frequency of Heavy Precipitation

Figure 6 provides a comparative analysis of monthly heavy precipitation occurrences between the study period of 2018-2022 and the long-term span from 1986 to 2015. Notably, the dry season months of January and February exhibit minimal occurrences, while October shines with an average of 9.1 events during the long-term period. However, a significant increase in heavy precipitation occurrences in the 2018-2022 period. During the flooding season, September and October take center stage, showcasing monthly averages of 7.6 and 10.2 events, respectively. This shift underscores a heightened prevalence of heavy precipitation events during flooding season compared to the long-term trend.

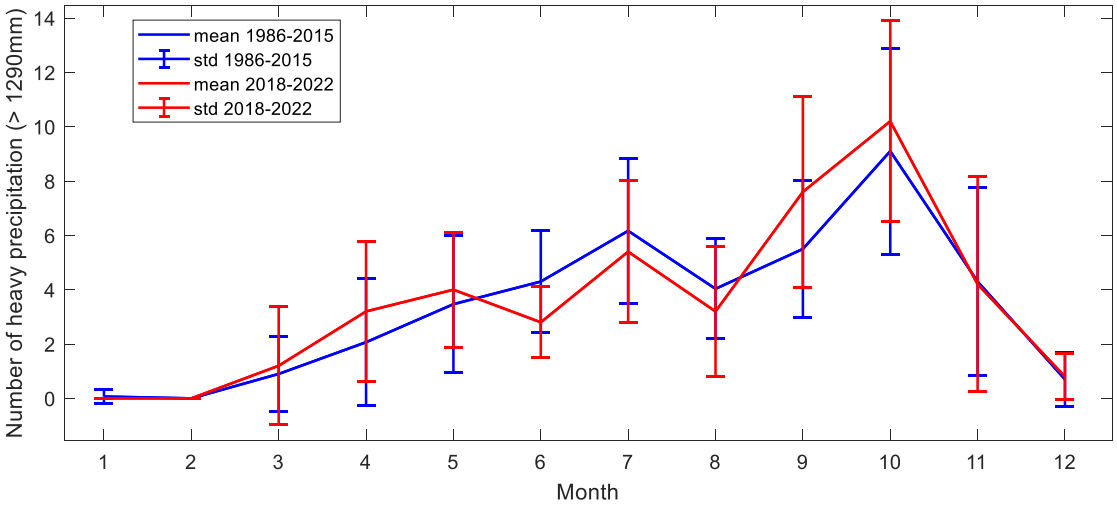

Figure 6. Monthly distribution of heavy precipitation events (daily rain volume > 1290mm) - A Comparison between the 2018-2022 period (shown in red) and the 30-year long-term period (1986-2015, shown in blue). The bars depict the standard deviation of heavy precipitation occurrences for each month within these respective timeframes.

To assess the significance of these changes, this study examined the frequency of heavy precipitation events over the crucial flooding months of August through November. Results reveal that the long-term 30-year period averaged approximately 22.9 events per year, while the five-year study period recorded a higher frequency of approximately 25.2 events per year. This indicates a discernible increase of around 10% in heavy precipitation events over the recent five years compared to the long-term 30-year period.

4.3 Flood Mapping

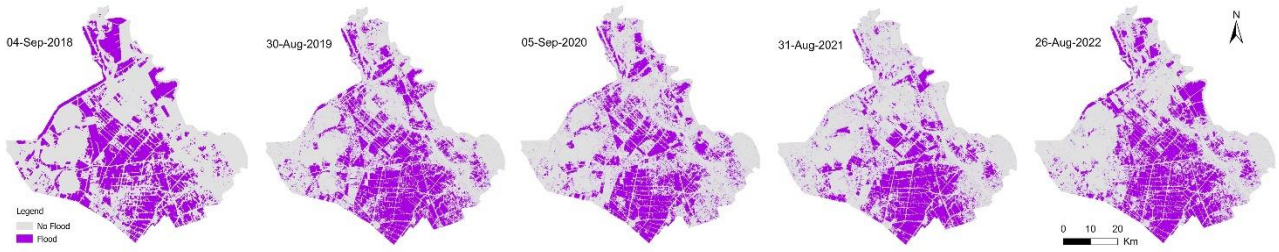

Figure 7. Flooding areas in An Giang province with the highest covering area in the year from 2018 to 2022: 04-September 2018, 30-August 2019, 05-September 2020, 31-August 2021, and 26-August 2022.

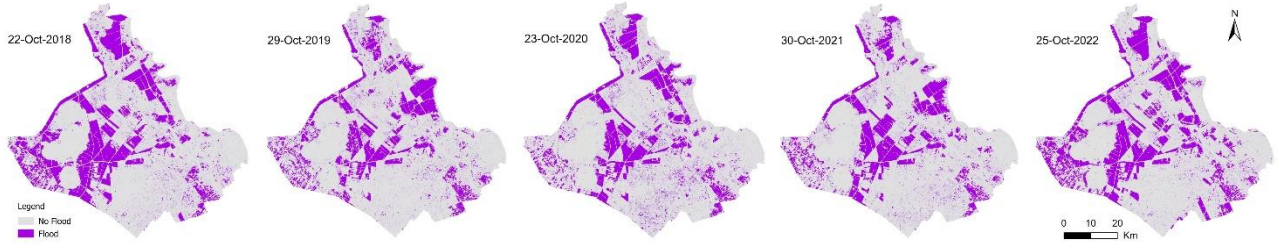

Figure 8. Flooding areas in An Giang province at the end of flood season in the year from 2018 to 2022: 22-October-2018, 29-October-2019, 23-October-2020, 30-October-2021, and 25-October 2022

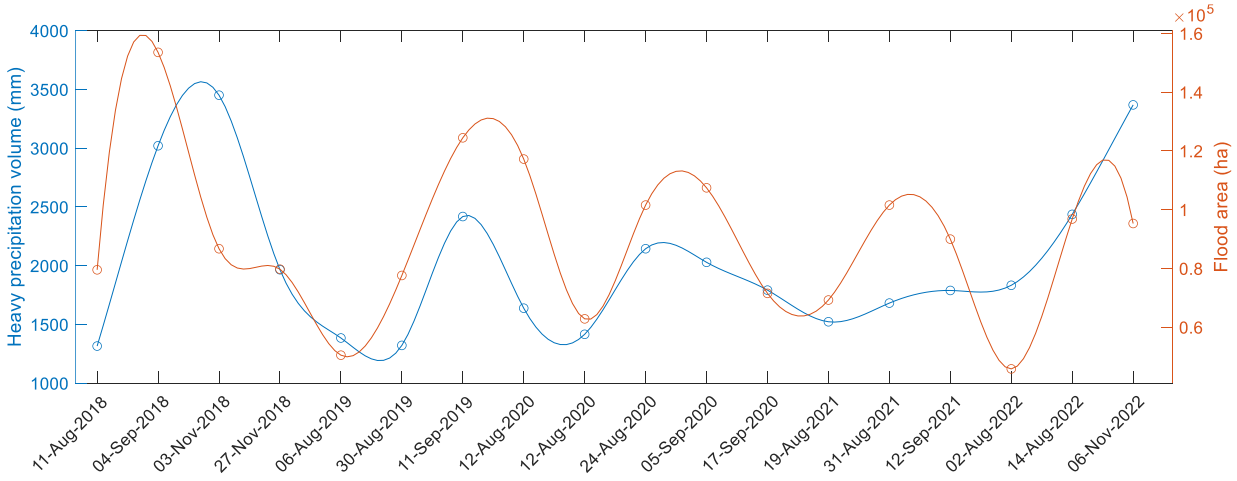

Figure 9. Heavy precipitation volume (blue line) and flood area (red line) in the 2018-2022 period

Figure 9 shows the heavy precipitation volume (represented as blue line) and flood area (represented as red line) from August 2018 to November 2022 in An Giang province. There seems to be a correlation between heavy precipitation events and subsequent flooding. For instance, on September 3, 2018, there was a heavy rainfall event with 3,019.5 mm of rain, and on the following day, September 4, 2018, witnessed a significant flood covering 153,503.9 hectares. By examining the data, it's evident that flood areas vary significantly, with some flood events covering vast areas (e.g., November 3, 2018, with 86,658.6 hectares) and others relatively smaller (e.g., August 06, 2019, with 50,423.0 hectares, August 2, 2022, with 45,751.8 hectares). These variations suggest that factors beyond precipitation volume, such as land use and drainage systems, may play significant roles in determining the extent of flooding.

Table 1: Heavy precipitation dates and flood dates and areas in 2018-2022

Order	Heavy Precipitation		Flood	
	Date	Volume (mm)	Date	Area (Ha)
1	05-Aug-2018	1,314.8	11-Aug-2018	79,480.0
2	03-Sep-2018	3,019.5	04-Sep-2018	153,503.9
3	24-Oct-2018	3,449.8	03-Nov-2018	86,658.6
4	25-Nov-2018	1,964.6	27-Nov-2018	79,692.1
5	06-Aug-2019	1,383.4	06-Aug-2019	50,423.0
6	08-Aug-2019	1,320.5	18-Aug-2019	77,560.5
7	29-Aug-2019	2,417.1	30-Aug-2019	124,418.8
8	30-Aug-2019	1,637.1	11-Sep-2019	117,182.2
9	03-Aug-2020	1,414.9	12-Aug-2020	62,784.2
10	07-Aug-2020	2,143.1	24-Aug-2020	101,516.1
11	03-Sep-2020	2,027.4	05-Sep-2020	107,392.5
12	15-Sep-2020	1,790.7	17-Sep-2020	71,465.4
13	23-Aug-2021	1,521.6	19-Aug-2021	69,197.3
14	24-Aug-2021	1,680.6	31-Aug-2021	101,522.7
15	07-Sep-2021	1,788.0	12-Sep-2021	89,924.4
16	30-Nov-2021	1,832.0	02-Aug-2022	45,751.8
17	06-Aug-2022	2,435.6	14-Aug-2022	96,779.3
18	27-Oct-2022	3,367.3	06-Nov-2022	95,248.4

CONCLUSION

The CHIRPS data were used to show the graphical representation of monthly heavy precipitation in An Giang Province, Viet Nam. It not only offers valuable insights into escalating trends and variations in heavy precipitation but also hints at potential repercussions for regional inundation dynamics, local climates, and weather-related factors in the study area influenced by climate change. Under the pervasive influence of climate change, the frequency of heavy precipitation in An Giang has notably increased during the flooding season. The CHIRPS data emerges as a valuable tool for visualizing this phenomenon and furthering our understanding of the evolving climate dynamics impacting the region.

In conclusion, heavy precipitation events appear to be associated with flooding in the studied area, but the extent of flooding is influenced by various local factors. Further analysis is needed to understand the specific mechanisms that lead to flooding and hydrological modeling must be incorporated to unravel the precise contribution of heavy precipitation events to flooding in the study area.

REFERENCES

References from Journals:

Banerjee, A., Chen, R., Meadows, M., Singh, R. B., Mal, S., & Sengupta, D. (2020). An Analysis of Long-Term Rainfall Trends and Variability in the Uttarakhand Himalaya Using the Google Earth Engine. *Remote Sensing, 12*, 709. doi:10.3390/rs12040709

Dubey, S., Gupta, H., Goyal, M., & Joshi, N. (2021). Evaluation of precipitation datasets available on Google earth engine over India. *International Journal of Climatology, 41*. doi:10.1002/joc.7102

Funk, C., Peterson, P., Landsfeld, M., Pedreros, D., Verdin, J., Shukla, S., . . . Hoell, A. (2015). The climate hazards infrared precipitation with stations—a new environmental record for monitoring extremes. *Scientific data, 2*(1), 1-21.

Jonkman, S. N. (2005). Global perspectives on loss of human life caused by floods. *Natural Hazards, 34*(2), 151-175.

Lehner, B., & Grill, G. (2013). Global river hydrography and network routing: baseline data and new approaches to study the world's large river systems. *Hydrological Processes, 27*(15), 2171-2186.

Lehner, B., Verdin, K., & Jarvis, A. (2008). New global hydrography derived from spaceborne elevation data. *Eos, Transactions American Geophysical Union, 89*(10), 93-94.

Pekel, J.-F., Cottam, A., Gorelick, N., & Belward, A. S. (2016). High-resolution mapping of global surface water and its long-term changes. *Nature, 540*(7633), 418-422.

References from Other Literature:

C2ES. (2023). Extreme Precipitation and Climate Change. Retrieved from https://www.c2es.org/content/extreme-precipitation-and-climate-change/

EPA. (2023, July 21, 2023). Climate Change Indicators: Heavy Precipitation. Retrieved from https://www.epa.gov/climate-indicators/climate-change-indicators-heavy-precipitation

Kramer, H. (2018, July 21, 2023). Copernicus: Sentinel-1–the sar imaging constellation for land and ocean services. Retrieved from https://www.eoportal.org/satellite-missions/copernicus-sentinel-1-2021#copernicus-program-ground-segment.